PROCEEDINGS OF SPIE REPRINT

SPIE—The International Society for Optical Engineering

Reprinted from

Optical Diagnostics for Fluids/Heat/Combustion and Photomechanics for Solids

21–23 July 1999
Denver, Colorado

Volume 3783

Application of imaging techniques to the study of vortex-flame interactions

Gregory J. Fiechtner,[a,b*] Paul-Henri Renard,[c] James R. Gord,[a]
Keith D. Grinstead, Jr.,[a,b] Campbell D. Carter,[a,b] and Juan Carlos Rolon[c]

[a]Air Force Research Laboratory, Propulsion Sciences and Advanced Concepts Division,
Wright-Patterson Air Force Base, OH 45433-7103, USA
[b]Present Address: Innovative Scientific Solutions, Inc., 2766 Indian Ripple Road,
Dayton, OH 45440-3638, USA
[c]Laboratoire d'Énergétique Moléculaire et Macroscopique, Combustion,
École Centrale Paris and CNRS, Grande Voie des Vignes
92295 Châtenay-Malabry Cedex, France

ABSTRACT

A thorough understanding of turbulent reacting flows is essential to the continued development of practical combustion systems. Unfortunately, these studies represent a tremendous research challenge owing to the inherent complexity of such flows. In an effort to reduce the complexity of these systems while capturing the essential features that define the physics and chemistry of turbulent reacting flows, we have been studying the interaction of a vortex with a laminar flame. The experimental apparatus includes a piston-cylinder device configured to provide a controlled toroidal vortex. The generated vortex/jet interacts with a nonpremixed hydrogen-air flame supported in a counterflow burner. The counterflow configuration permits precise selection of the flame and the associated strain field. Vortex characterization is essential to interpreting the experimental observations and accomplishing numerical modeling of vortex-flame interactions. Two-color particle-image velocimetry (PIV) has been employed to characterize the vortex and to describe the underlying counterflow velocity field. The hydroxyl (OH) layer produced by the flame is imaged using planar laser-induced fluorescence (PLIF). The PIV and PLIF measurements of OH are performed simultaneously. A distinct annular extinction of the OH layer is observed, in good agreement with previous computational modeling predictions for the apparatus.

Keywords: PIV, PLIF, Laser-Induced Fluorescence, Vortex, Turbulence, Combustion

1. INTRODUCTION

Recent results in numerical modeling combined with experimental measurements have led to important advances in the understanding of combustion. Numerous investigations have contributed to these advances, including a particular type of study in which the interaction of a laminar, nonpremixed flame and a vortex is examined. These efforts involve repeatable, carefully controlled conditions that are highly amenable to experimental study. The resulting data can be used for a variety of purposes, such as identifying fundamental regimes of vortex-flame interactions.[1] Vortical structures are an important feature in unsteady and turbulent combustion,[2-5] and experimental data can be used to develop models for use in practical combustion topics such as experimental gas turbine combustors.[6-9] This paper contains experimental results that are used to validate prior numerical computations.

In recent computational calculations, Katta[10] predicted that during the interaction of a nonpremixed hydrogen-air flame and an isolated vortex, the extinction of the OH layer would occur in an annular pattern. The experiments detailed in the present paper are performed to examine, in part, the validity of this prediction. Experimental results obtained with planar laser-induced fluorescence (PLIF) of OH are used to determine regimes in which the annular extinction occurs. The nonpremixed flame is supported by air and fuel in an opposed-jet burner. The fuel consists of hydrogen diluted with nitrogen. The temporal evolution of the vortex-flame interactions is imaged with the PLIF system. Additional measurements are performed to characterize the vortices. Particles are seeded into the flowfield, and the scattering is used for digital, two-color particle-image velocimetry (PIV) measurements. Digital PIV measurements are made simultaneously with PLIF measurements of OH.

* Further author information: (Send correspondence to G.J.F.)
G.J.F.: E-mail: gjfiech@ward.appl.wpafb.af.mil, Tel: (937) 255-8373, WWW: www.innssi.com

Part of the SPIE Conference on Optical Diagnostics for Fluids/Heat/Combustion
and Photomechanics for Solids • Denver, Colorado • July 1999
SPIE Vol. 3783 • 0277-786X/99/$10.00

An annular break in the OH layer is observed, in agreement with the predictions of Katta using numerical computations.[10] The annular pattern is accompanied by comparatively large flame curvature. The temporal resolution that is necessary to resolve the annular break experimentally is found to agree with the magnitude of the computational time step used by Katta.

2. BACKGROUND

Numerous experimental studies of the interaction dynamics of vortices and flames have been conducted, and many of these investigations employed two-dimensional imaging to study the interaction. For premixed flame fronts, most measurements have been made using two types of flames. Hertzberg et al.[11] and Escudie[12] conducted an experiment in which a Karman vortex street was produced using a cylindrical rod in a cross flow of premixed gases. A V-flame was supported behind a wire positioned downstream of the rod that produced the vortex street. Planar tomographic imaging was used to study the interaction of the vortex street and the flame. A similar interaction of a Karman vortex street and a flame was investigated by Lee et al.[13] using PLIF imaging of OH and by Nye et al.[14] using both OH PLIF and PIV. A disadvantage of using the vortex street is the difficulty in isolating a single vortex. Samaniego[15] developed a means of injecting an isolated line vortex through a horizontal slot in the wall of a vertical wind tunnel; this was pursued as a means of replacing the vortex street in experiments with V-flames. A year later, Samaniego[16] presented results on the interaction of a line vortex and a V-flame. Schlieren images of the time-dependent vortex-flame interaction along with CH emission data from the entire flame were presented. Nguyen and Paul[17] also studied vortex-flame interactions using the Samaniego burner, reporting results of PLIF measurements of OH and CH radicals.

In a second type of study involving premixed combustion, Jarosinski et al.[18] studied a flame that was ignited at one end of a tube of premixed gases. A vortex was injected at the other end of the tube. The interaction dynamics were then photographed using a mercury-xenon arc lamp and a rotating-drum streak camera with a rotating-disc shutter. Recently, Driscoll and co-workers produced an impressive series of papers concerning a similar vortex-flame facility in which PIV, OH PLIF, or a combination of these imaging techniques was applied.[19-27]

Nonpremixed flames have also been the subject of experimental study. Rolon and co-workers[1,28-31] recently developed an apparatus in which a vortex is injected into a flame supported between the nozzles of an opposed-jet burner. This geometry has numerous advantages. First, unlike the above geometries, a stationary nonpremixed flame can be produced and isolated easily. Second, the flame thickness can be varied by changing either the nozzle velocities or the spacing between the upper and lower burner nozzles. The device has also been extended to the study of vortices that interact with premixed opposed-jet flames.[1] Takagi and coworkers[32,33] performed planar Rayleigh-scattering measurements of temperature in a similar type of opposed-jet burner in which a small jet of fuel or air was injected using a micro nozzle with an inner diameter of only 0.25 mm. Either a jet of air was injected from the air side of the diffusion flame or a jet of fuel was injected from the fuel side. Santoro and coworkers[34] modified a vortex counterflow burner so that either gaseous or spray flames can be studied.

In a different class of measurements, Hsu et al.[35,36] modulated the axial velocity of a laminar jet diffusion flame using a loud speaker to produce vortex-flame interactions. This apparatus was further studied by Hancock and coworkers[37] using a number of techniques including reactive Mie scattering, PLIF, and digital PIV. These studies have provided large quantities of data for comparison with numerical-modeling predictions. A potential disadvantage of this burner is the complicated geometry (when compared to the above geometries, which involve completely isolated vortex injection) due to the convective velocity field associated with rotation of the vortex and translation of the flame zone. In a similar type of study, Mueller and Schefer[38] performed OH PLIF measurements in a Wolfhard-Parker slot burner that was forced acoustically by loud speakers on the side walls of the upstream fuel duct. PLIF imaging of acetone was used as a marker of the fuel.

More recently, Chen and Dahm[39] developed a facility for generating a nonpremixed burning layer that wraps into a vortex ring. The facility has been operated under conditions of both normal gravity and microgravity, allowing the study of the influence of buoyancy. In contrast, You et al.[40] have designed a facility in which the vortex is ignited just as the fluid begins to exit a tube.

The experiments described in the present paper are based on the counterflow geometry of Rolon and co-workers.[1,28-31] A fuel mixture of hydrogen and nitrogen permits the use of laser diagnostics in the absence of hydrocarbon interferences. Hydrogen chemistry simplifies the numerical calculations that are the subject of comparison with experimental results.[2,3,10,41]

3. APPARATUS AND PROCEDURE

3.1 Burner Facility

A picture (a) and diagram (b) of the Rolon burner are shown in Figure 1. The flame is supported between upper and lower nozzles separated by 40 mm, each with an exit diameter of 25 mm. The fuel consists of hydrogen diluted with nitrogen and flows from the upper nozzle. Air flows from the lower nozzle. Unique to this type of apparatus is a tube with 5-mm inner diameter that is installed concentrically within the lower nozzle. This tube is attached to a cylinder that contains a piston which, in turn, is attached to an actuator. Feeding an appropriate current to the actuator causes a solenoid to force the piston upward abruptly, resulting in the emergence of a vortex from the tube. For a cylindrical volume of fluid that emanates from a nozzle having length L and diameter D, Gharib et al.[42] have shown that the maximum circulation which a vortex ring can attain is reached for L/D at ~4 and that for larger ratios additional trailing vortex rings form. For the present 0.5-cm nozzle, the volume that a vortex can contain as estimated from the results of Gharib et al.[42] is ~0.4 cm^3. The present vortex generator can sweep a maximum volume of ~3 cm^3, for a maximum attainable L/D ratio of ~30. For the experiments described in this paper, comparatively strong vortices are generated using a 0.1-ms piston risetime. The piston is allowed to travel through its maximum range, but the tube is placed such that the diagnostics are triggered before a secondary or tertiary vortex exits the tube. This process is illustrated in Figure 2. In frame 1 of Figure 2, a slug of fluid begins to exit the tube, while in frame 2, the vortex begins to form. After frame 2, one of two paths is followed depending on the motion of the piston. If the piston is stopped (path A), the vortex pinches off as it travels upward, as illustrated in frames 3A and 4A of Figure 2. If the piston motion is allowed to continue (path B), the vortex travels initially above a column of fluid, as shown in frame 3B. This condition is selected for the present experiments because the resulting vortex resembles closely the corresponding vortices used in the computations of Katta.[2,3,41] Therefore, models that rely on an artificially created vortex pair by specifying the vortex field may not be well-represented by our experimental conditions.[43] If the piston is allowed to pump fluid from the nozzle at later times, multiple vortices can be produced from the tube, as illustrated in frame 4B of Figure 2. Vortex conditions are monitored carefully by examining scattering images acquired with a color digital camera; the multiple-vortex condition is avoided in this manner. It is also possible for vortices that are initially laminar to then become unsteady and turbulent,[44] conditions that are carefully avoided. In addition, if the piston/cylinder is not properly aligned and lubricated, an undesired turbulent puff of fluid exits the tube.[45,46]

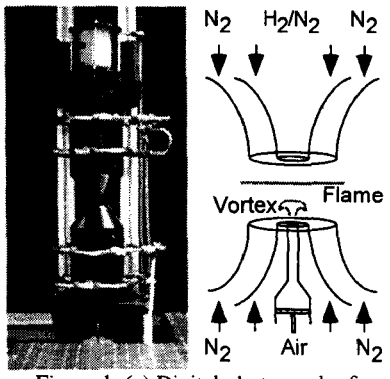

Figure 1. (a) Digital photograph of opposed-jet burner. (b) Cross-sectional diagram of burner nozzles and piston.

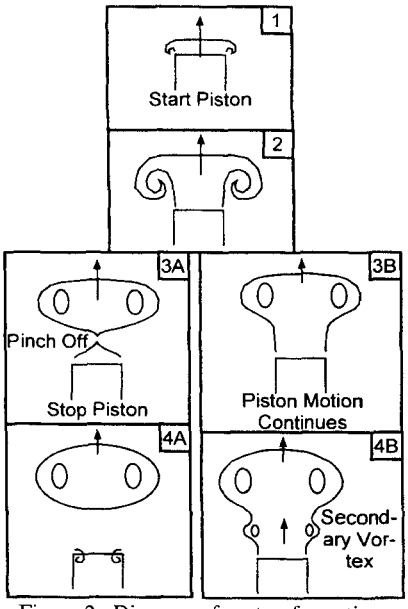

Figure 2. Diagram of vortex-formation processes.

The laminar vortices travel upward within the surrounding oxidizer flow. A flow of air is supplied to the vortex tube such that in the absence of a vortex, the exit velocity matches the velocity of the air from the surrounding nozzle. To minimize the impact of room-air disturbances, upper and lower guard flows of nitrogen are supported through outer nozzles, which are concentric with the respective upper and lower inner nozzles that support the flame. The hydrogen, nitrogen-diluent, and oxidizer-air flows are furnished by mass-flow controllers with respective full-scale ranges of 20, 20, and 30 l/min. A continuous flow of air is provided to the vortex tube by a 5-l/min controller, while the guard flows for the upper and lower guard (outer) nozzles are furnished by two 50-l/min mass-flow controllers. The flow rates of the controllers are accurate to ±1% of the full-scale range. The experiments have been completed for a volume fraction of H_2 in N_2 of 0.19, with flow rates for H_2, N_2, and Air of 4.04, 17.1, and 11.2 l/min, respectively.

Seed particles are introduced into the burner flows when digital PIV measurements of the vortex velocity are performed. Three particle seeders are installed; one is placed after the air mass-flow controller, another after the vortex-air mass flow controller, and a third after the junction where the hydrogen and nitrogen gases are mixed. With the use of three seeders, each flow can be seeded with particles individually, or combinations of the different flowfields can be seeded. Each seeder

contains hollow spherical ceramic particles with an approximate mean diameter of 2.4 μm. When PIV studies are not required, the seeders are removed from the apparatus. Experiments are repeated for both seeded and unseeded flows, and no significant change in the results is caused by the presence of seed particles.

3.2 Synchronization and Timing

The time-dependent nature of vortex-flame interactions is compared to computational predictions. Precise synchronization of several experimental events is required, including vortex generation and propagation, production of laser pulses, and activation of the camera shutter and intensifier. A block diagram of the synchronization scheme is included in Figure 3.

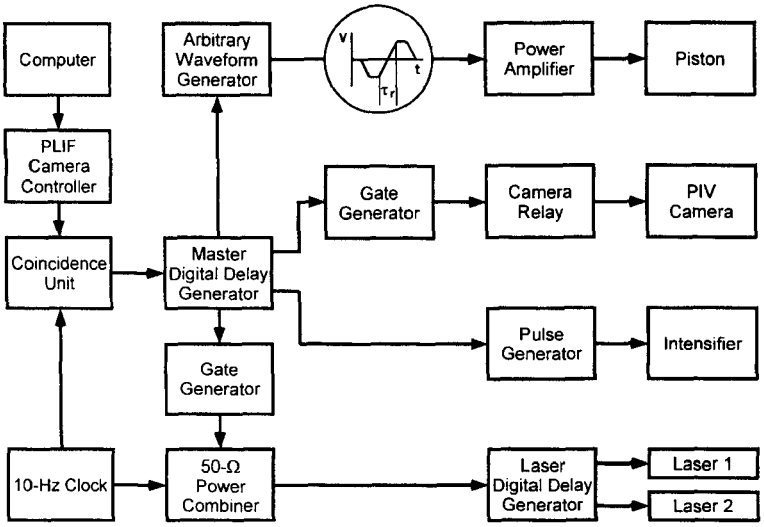

Figure 3. Diagram of electronic timing connections for simultaneous OH PLIF and digital PIV measurements.

Because the Nd:YAG lasers are designed to operate at a nominal repetition rate of 10 Hz, the experimental sequence must be synchronized to a 10-Hz master clock that drives the flash lamps and the Pockels cells of the lasers. To trigger the lasers, the clock sends two signals—one traveling to a 50-Ω power combiner and then to the laser digital delay generator (DDG). The 10-Hz clock also provides a TTL signal to one of two inputs of a coincidence unit. The second input of this unit is driven by a TTL pulse from the PLIF camera controller. The coincidence unit outputs a pulse only when pulses from both the 10-Hz clock and the PLIF camera controller are present. When a vortex-flame event is initiated using a personal computer, the PLIF camera controller outputs a pulse ~1.3 s in duration. The corresponding output of the coincidence unit is a 1.3-s envelope of TTL pulses separated by 100 ms. The first pulse in this envelope triggers a master DDG, synchronizing it with the 10-Hz clock and the laser pulse train. This DDG triggers an arbitrary-waveform generator (AWG) that outputs a 1-s waveform; this waveform is amplified and fed to the piston actuator to generate a vortex. Approximately 0.5 s after the AWG waveform is initiated, the vortex is fired; therefore, five laser pulses are generated during the time between computer initiation and the vortex-flame interaction.

When the DDG is externally triggered, the jitter between the trigger and a DDG output pulse is 60 ps plus the output delay divided by 10^8. Over the 0.5-s period between the first and fifth laser pulses, this corresponds to a jitter of 5.06 ns. The 10-Hz-clock jitter specifications are not nearly so good. The jitter between clock outputs is one part in 10,000, corresponding to a jitter of 50 μs over the same 0.5-s period. Attempting to synchronize the piston with the clock limits the temporal resolution available to "freeze" vortex-flame events in time and requires an intensifier gate width significantly larger than 50 μs. The master DDG is, therefore, configured to trigger the fifth laser pulse preemptively. A delayed pulse from the master DDG arrives at the 50-Ω power combiner just before the fifth pulse in the clock pulse train, triggering the laser(s) preemptively. If no initiation pulse is output from the computer, the laser(s) are triggered by the 10-Hz clock as usual. This approach reduces the jitter in the timing of the fifth laser pulse from 50 μs to ~5 ns while maintaining the nominal 10-Hz repetition rate required by the lasers.

Other outputs of the master DDG are delayed suitably and directed to the image detectors. For PIV experiments, the width of a TTL pulse is adjusted using a gate generator, which closes a relay to trigger the digital PIV camera system. For simultaneous PLIF experiments, another master-DDG output triggers a pulse generator which, in turn, activates the intensifier of an ICCD camera.

The scheme depicted in Figure 3 provides precise control of the relative timing between the laser diagnostics and the vortex-flame event. To explore the temporal evolution of the event, data are captured utilizing the following phase-locked timing sequence: 1) an image is recorded, 2) the delay between vortex production and the laser/camera events is adjusted, and 3) another vortex is initiated and a second image recorded. This process is repeated to acquire numerous images, obtained at increasing delays. Effective temporal separation between images is selected between 10 and 3 ms, depending on

the time scale of the event under study. The resulting temporal sequences of images are a testament to the high degree of repeatability achievable with this apparatus.

3.3 Measurement Techniques and Data Collection

The PLIF system contains a frequency-doubled, Q-switched Nd:YAG laser that is used to pump a dye laser which, in turn, is frequency doubled. The UV radiation is directed through a telescope that is adjusted to produce a light sheet with a height that matches as nearly as possible the 40-mm burner separation. The resulting beam thickness is ~300 μm, which corresponds to the full width (defined as the distance between the locations of the 25% peak intensity points).

Hydroxyl radicals absorb the laser radiation at 281.3414 nm via the $R_1(8)$ transition of the (1,0) band in the A-X system. Fluorescence from the A-X (1,1) and (0,0) bands is detected at right angles through WG-295 and UG-11 colored-glass filters, using a 105-mm-focal-length f/4.5 UV lens. The resulting light is recorded on an intensified CCD camera with an intensifier gate width of 100 ns. CCD pixels are binned in 2 x 2 groups, resulting in an effective array size of 288 x 192 pixels, with an imaged area of 25.6 x 38.4 mm^2. The images are cropped such that the bottom of each image coincides with the top surface of the lower nozzle. A color table is used with a maximum value set to 95% of the maximum signal for all images taken at a given flame condition. The low-signal color is assigned by calculating the background noise and selecting a minimum value that is two standard deviations above this level. Therefore, in cases where "extinction" of the OH layer is observed, "extinction" refers to signal levels that fall below this minimum value and are, therefore, assigned the last color in the table. The last color is chosen to be white to facilitate easy viewing of images when overlayed with velocity vectors.

In studies of vortex-flame interactions conducted by other investigators (see, for example, Najm et al.[47,48]), PLIF was applied as a marker of some other quantity such as heat release or burning rate. In the present experiments, the OH image is obtained for direct comparison with numerical computations of the OH distribution with respect to certain spatial features;[10] therefore, no attempt is made to correlate the images with any other quantities, although it has been shown recently that the OH concentration may be a good indicator of flame extinction in this configuration.[28] The presence of a break in the OH layer is ascertained by repeating measurements at later delays, for which it is obvious that the vortex passes through a hole in the flame zone. We do not attempt to map the detailed OH concentration profiles across the flame zone in the vicinity of the perceived break.

Measurements of the velocity field are carried out using digital, two-color PIV.[49,50] Here, a color digital CCD with an array of 3060 x 2036 pixels is used. A magnification of 78,368 pixels/m is employed, resulting in an imaged area of 26.0 x 39.0 mm^2. The color CCD camera and the intensified CCD array are aligned using a transparent mask printed with a graduated scale. Further alignment between images is performed after each experiment employing software; a transformation in two-dimensional space is applied to the PIV images relative to the PLIF images. Two lasers are used, with one PIV light sheet produced by doubling the output of a Q-switched Nd:YAG laser directly (30 mJ/pulse at the test section). The remainder of this beam is used to pump the dye laser that is frequency doubled to excite OH fluorescence. The second PIV light sheet is produced by pumping a dye laser (employing DCM laser dye) with a second frequency-doubled, Q-switched Nd:YAG laser, resulting in laser radiation at 640 nm (40 mJ/pulse at the test section). The thickness of both the red and green light sheets is set to ~700 μm at the probe region. A digital delay generator is used to drive the timing of the two lasers such that the red pulses are delayed precisely with respect to the green ones. In the absence of a vortex, the underlying counterflow velocity field is probed with red pulses that are delayed by up to 1 ms with respect to the corresponding green pulses. For the fastest vortices studied, the delay between red and green pulses is reduced to 10 μs. The camera shutter is set to open for 1/15 s to permit both laser pulses to be detected by the color CCD. Most of the flame emission and light from other devices in the laboratory (monitors, etc.) is greatly attenuated by the shutter.

Velocity vectors are calculated using the correlation software described by Gogineni and coworkers.[49,50] A correlation area of 128 x 128 pixels is used in the calculation, corresponding to a correlation area of 0.269 cm^2 and a spatial resolution of 1.6 mm. The digital PIV measurements are performed to obtain the propagation velocity of the vortex to match experimental and computational conditions; this correlation area is acceptable for such purposes. Neighboring correlation boxes are overlapped by 75%, resulting in a velocity field with an area containing 95 x 60 vectors, or 5700 total vectors over the area of the color CCD. In some portions of each image, a small percentage of errant vectors results from low seed levels, scattering of light into the camera, flame emission, and other effects. Because the vortex-flame interactions are repeatable, digital PIV images can be recorded until an image with an extremely small percentage of incorrect vectors is obtained. For presentation purposes, most vectors are not plotted, with fields of 15 x 32 vectors selected for the present images.

Color digital images acquired using the PIV system can also be used without further computation of velocity vectors. By adjusting the seed level in the vortex-tube flow so that it is either noticeably larger or smaller than the seed levels for the rest

of the burner, flow visualization of the vortex-formation process is possible. Because of the temporal separation between the red and green laser pulses, these images may appear to be slightly blurred.

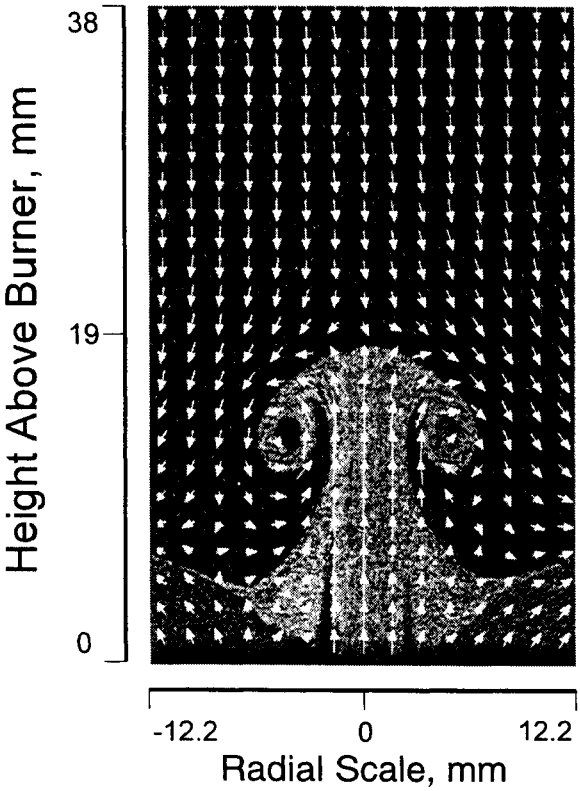

Figure 4. Scattering from particles in vortex flow with PIV velocity field superimposed.

4. RESULTS AND DISCUSSION

The scattering image of Fig. 4 is obtained when the vortex-tube flow is seeded with a slightly higher particle density than that produced by the upper and lower burners. As shown, the "mushroom" vortex advances ahead of a column of fluid because the piston continues to push fluid from the vortex nozzle. The fluid column takes on the appearance of the stem of a mushroom. The scattering image of Fig. 4 is taken in a cold flow. Vortices produced in reacting flows also exhibit the laminar stem-like appearance in the wake. The vortex has a propagation velocity of 1.5 m/s.

The PLIF images of OH shown in Figure 5 correspond to a vortex-flame interaction in which extinction of the OH layer is not observed. Initially, the vortex creates a small dent in the flame, and this dent begins to grow. Eventually the flame engulfs the advancing vortex as it approaches the upper nozzle. The vortex of Figure 5 has a propagation velocity of 3.9 m/s.

The images of Figure 6 correspond a vortex that has a propagation velocity of 5.0 m/s. Extinction of the OH layer is observed. After extinction the vortex travels upward toward the other nozzle. The flame follows the vortex, traveling up the stem. The temporal resolution of the sequence plotted in Figure 6 is not sufficient to observe the local structure of the extinction of the OH layer. We have found that a temporal resolution of 10 μs is often necessary to study these regimes adequately for hydrogen/air flames.[51] This temporal resolution agrees with the resolution used by Katta[10] during numerical simulations of these interactions. An image of the spatial structure taken at the instant of extinction of the OH layer is shown in Figure 7. The annular break in the OH layer was first predicted numerically by Katta[10] attesting to the utility of his code. The annular pattern is also observed in experiments in which Rayleigh scattering images of temperature are recorded.[51]

5. FUTURE INVESTIGATIONS

The Rolon burner may prove to be ideal for studying other interactions of importance to combustion. One example that we have recently begun to study is the behavior of fire suppressants injected into a laminar hydrocarbon flame. Here, the vortex-injection tube is fitted with a three-way solenoid valve having two inlets. The first inlet provides the air flow described in this paper. The second inlet provides some other gas mixture or a droplet-containing flow. The current to the solenoid valve is timed such that it switches to the second inlet only for a period of time sufficient to fill the vortex tube. The piston is then triggered to produce a carefully-controlled vortex or jet. The interaction with the flame is monitored using the diagnostics described in this paper.

Measurement techniques are being improved to aid in interpretation of the data. For example, simultaneous acquisition of PLIF and PIV data enables careful examination of quantities such as flame stretch by overlapping images from two cameras. Vectors were calculated using an effective spatial resolution of ~1.6 mm, which may be inadequate for spatial derivatives in the vicinity of the flamefront. We are presently working to improve the spatial resolution. More importantly, thermophoresis may introduce a bias into velocity vectors where temperature gradients are large.[52,53] Using simultaneous PLIF and Rayleigh-scattering measurements of temperature, we hope to use overlapped flame fronts to overlap corresponding velocity and temperature fields. The resulting images should permit an examination of thermophoretic bias on the velocity field.

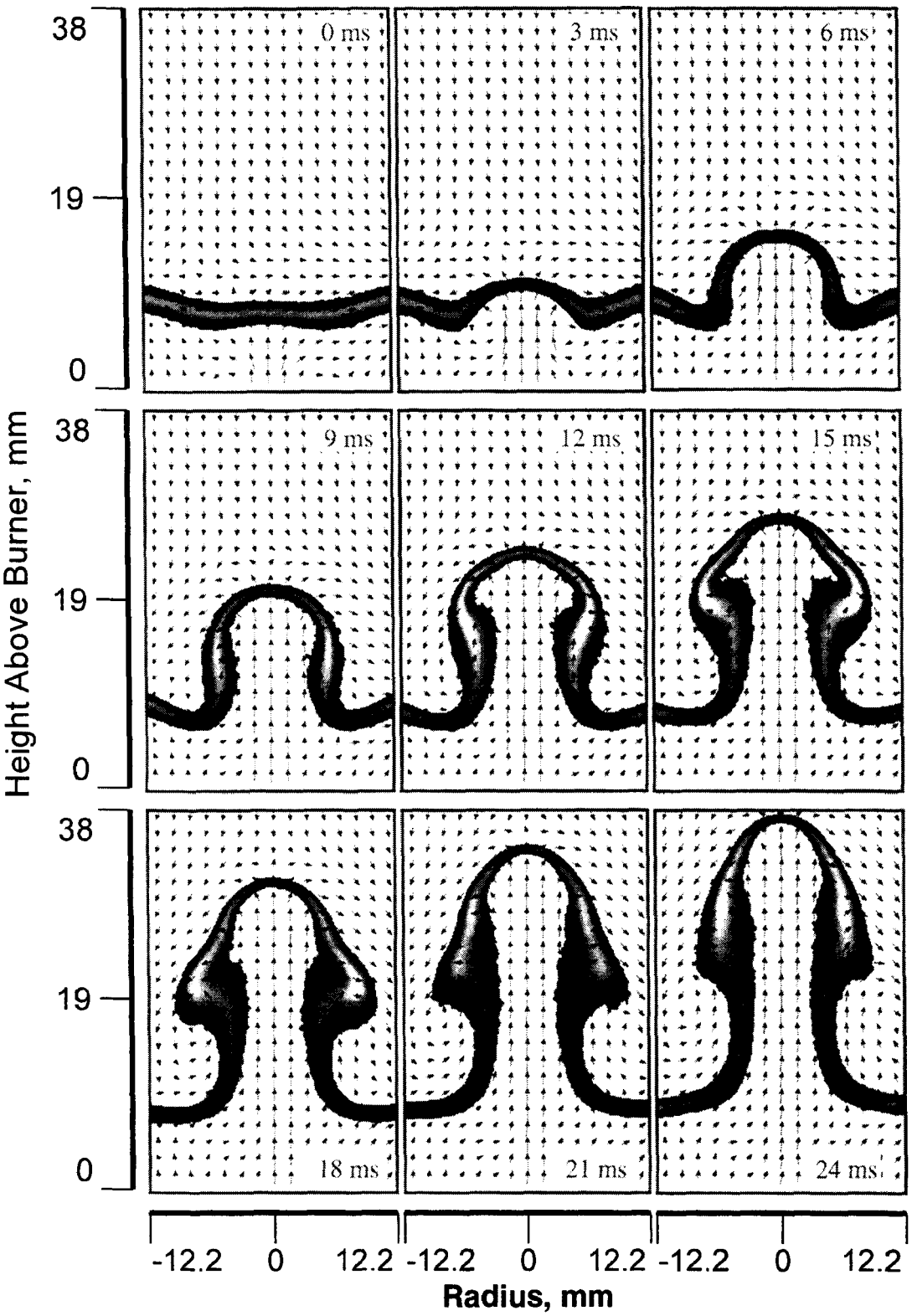

Figure 5. Sequence of PIV/OH PLIF images taken when the OH layer remains intact.

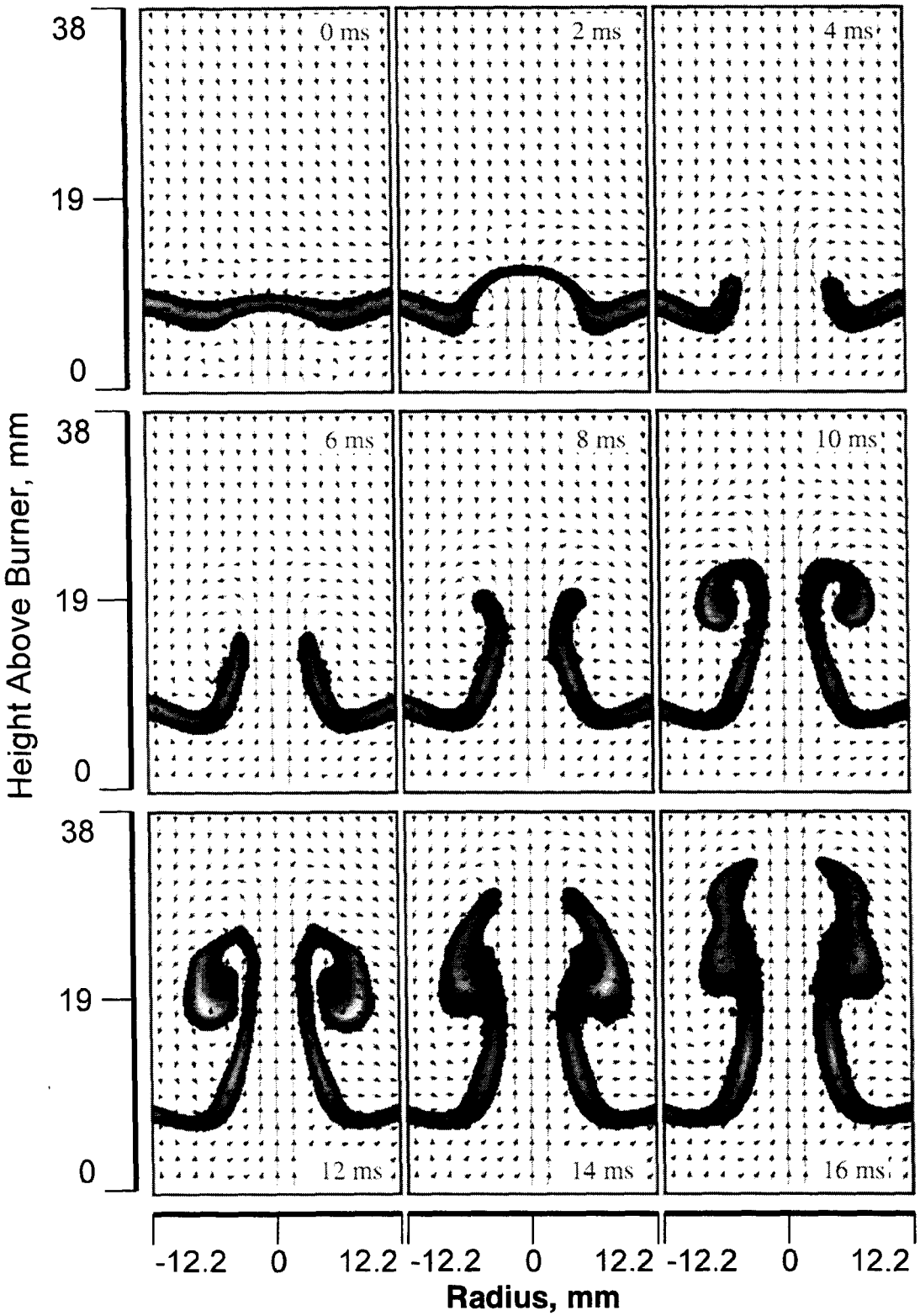

Figure 6. Sequence of PIV/OH PLIF images taken before and after local extinction of the OH layer.

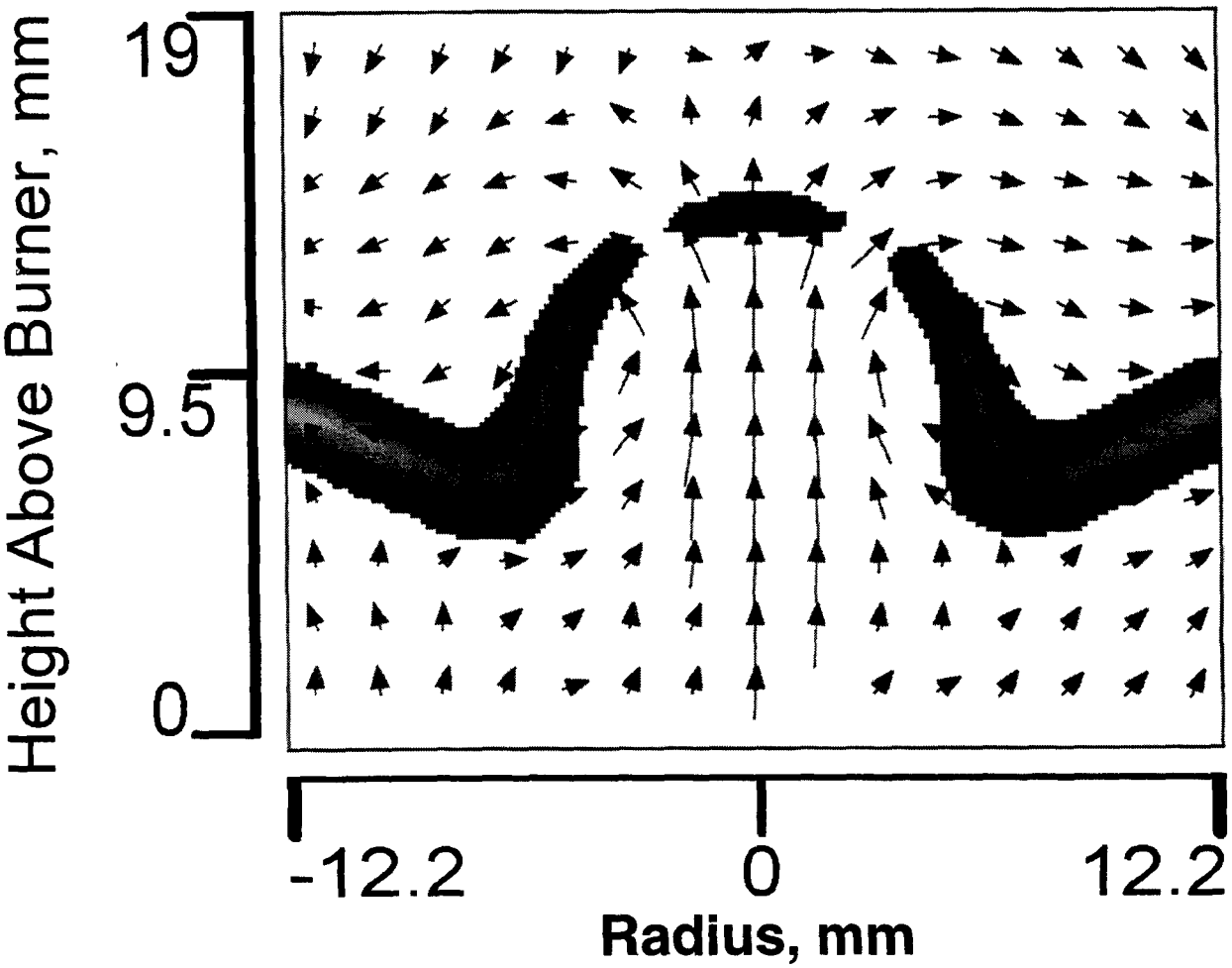

Figure 7. PIV/OH PLIF image of the annular extinction of the OH layer.

6. CONCLUSIONS

The apparatus of Rolon and co-workers[1,28-31] has been implemented to study the interaction of a vortex and a flame. Digital two-color PIV has been applied to characterize the vortices injected into the opposed-jet flow. Simultaneous PLIF images of OH have been used to observe the dynamics of the interaction of the vortex and the flame. An annular break in the OH layer has been observed, in excellent spatial and temporal agreement with the numerical computations of Katta.[10]

ACKNOWLEDGEMENTS

The authors thank Dr. J. M. Donbar for technical assistance in setting up the experiments. The authors also acknowledge the advice of Drs. L. P. Goss, S. P. Gogineni, J. Estevadeordal, M. A. Linne, and Mr. T. Drouillard concerning the reduction of two-color PIV data. The authors thank Dr. R. D. Hancock and Lt. I. Vihinen for assistance in assembly and construction of the burner. The authors also acknowledge Drs. J. M. Donbar, R. D. Hancock, W. M. Roquemore, V. R. Katta, and K.-Y. Hsu for the stimulating discussions of vortex-flame dynamics. Finally, the authors wish to thank Ms. M. M. Whitaker for editorial assistance. This work is supported by U. S. Air Force Contracts F33615-95-C-2507 and F33615-97-C-2702.

REFERENCES

1. P.-H. Renard, J. C. Rolon, D. Thevenin, and S. Candel, "Wrinkling, Pocket Formation and Double Premixed Flame Interaction Processes," *Twenty-Seventh Symposium (International) on Combustion*, The Combustion Institute, Pittsburgh, PA, pp. 659-666, 1998.
2. W. M. Roquemore and V. R. Katta, "Role of Flow Visualization in the Development of UNICORN," *International Conference on Optical Technology and Image Processing in Fluid, Thermal, and Combustion Flow*, Yokohama, Japan, Paper No. KL-310, 1998.
3. W. M. Roquemore and V. R. Katta, "Role of Flow Visualization in the Development of UNICORN," *Journal of Visualization*, in press, 1999.
4. F. Takahashi, W. J. Schmoll, D. D. Trump, and L. P. Goss, "Vortex-Flame Interactions and Extinction in Turbulent Jet Diffusion Flames," *Twenty-Sixth Symposium (International) on Combustion*, The Combustion Institute, Pittsburgh, PA, pp. 145-152, 1996.
5. W. M. Roquemore, V. K. Reddy, P. O. Hedman, M. E. Post, T. H. Chen, L. P. Goss, D. Trump, V. Vilimpoc, and G. J. Sturgess, "Experimental and Theoretical Studies in a Gas-Fueled Research Combustor," *29th AIAA Aerospace Sciences Meeting*, Reno, NV, AIAA 91-0639, 1991.
6. V. R. Katta and W. M. Roquemore, "Numerical Studies on Trapped-Vortex Concepts for Stable Combustion," *Trans. ASME* **120**, pp. 60-68, 1998.
7. V. R. Katta and W. M. Roquemore, "Study on Trapped-Vortex Combustor--Effect of Injection on Dynamics of Non-Reacting and Reacting Flows in a Cavity," *33rd AIAA/ASME/SAE/ASEE Joint Propulsion Conference & Exhibit*, Seattle, WA, AIAA 97-3256, 1997.
8. M. D. Durbin, M. D. Vangsness, D. R. Ballal, and V. R. Katta, "Study of Flame Stability in a Step Swirl Combustor," *Trans. ASME* **118**, pp. 308-315, 1996.
9. K. Y. Hsu, C. D. Carter, V. R. Katta, and W. M. Roquemore, "Characteristics of Combustion Instability Associated with Trapped-Vortex Burner," *37th AIAA Aerospace Sciences Meeting and Exhibit*, Reno, NV, AIAA 99-0488, 1999.
10. V. R. Katta, C. D. Carter, G. J. Fiechtner, W. M. Roquemore, J. R. Gord, and J. C. Rolon, "Interaction of a Vortex With a Flat Flame Formed Between Opposing Jets of Hydrogen and Air," *Twenty-Seventh Symposium (International) on Combustion*, The Combustion Institute, Pittsburgh, PA, pp. 587-594, 1998.
11. J. R. Hertzberg, M. Namazian, and L. Talbot, "Tomographic Study of a Laminar Flame in a Karman Vortex Street," *Combust. Sci. Technol.* **38**, pp. 205-216, 1984.
12. D. Escudie, "Stability of a Premixed Laminar V-Shaped Flame," *Prog. Astronaut. Aeronaut.* **113**, pp. 215-239, 1988.
13. T.-W. Lee, J. G. Lee, D. A. Nye, and D. A. Santavicca, "Local Response and Surface Properties of Premixed Flames During Interactions with Karman Vortex Streets," *Combust. Flame* **94**, pp. 146-160, 1993.
14. D. A. Nye, J. G. Lee, T.-W. Lee, and D. A. Santavicca, "Flame Stretch Measurements During the Interaction of Premixed Flames and Karman Vortex Streets Using PIV," *Combust. Flame* **94**, pp. 167-176, 1996.
15. J.-M. Samaniego, "Generation of Two-Dimensional Vortices in a Cross Flow," *Annual Research Briefs--1992*, Center for Turbulence Research, NASA Ames Research Center/Stanford University, pp. 431-441, 1992.
16. J.-M. Samaniego, "Stretch-Induced Quenching in Vortex-Flame Interactions," *Annual Research Briefs--1993*, Center for Turbulence Research, NASA Ames Research Center/Stanford University, pp. 205-218, 1992.
17. Q.-V. Nguyen and P. H. Paul, "The Time Evolution of a Vortex-Flame Interaction Observed via Planar Imaging of CH and OH," *Twenty-Sixth Symposium (International) on Combustion*, The Combustion Institute, Pittsburgh, PA, pp. 357-364, 1996.
18. J. Jarosinski, J. H. S. Lee, and R. Knystautas, "Interaction of a Vortex Ring and a Laminar Flame," *Twenty-Second Symposium (International) on Combustion*, The Combustion Institute, Pittsburgh, PA, pp. 505-514, 1988.
19. J. F. Driscoll, D. J. Sutkus, W. L. Roberts, M. E. Post, and L. P. Goss, "The Strain Exerted by a Vortex on a Flame--Determined from Velocity Field Images," *Combust. Sci. Technol.* **96**, pp. 213-229, 1994.
20. C. J. Mueller, J. F. Driscoll, D. J. Sutkus, W. L. Roberts, M. C. Drake, and M. D. Smooke, "Effect of Unsteady Stretch Rate on OH Chemistry During a Vortex-Flame Interaction: To Assess Flamelet Models," *Combust. Flame* **100**, pp. 323-331, 1995.
21. C. J. Mueller, J. F. Driscoll, D. L. Ruess, and M. C. Drake, "Effects of Unsteady Stretch on the Strength of a Freely-Propagating Flame Wrinkled by a Vortex," *Twenty-Sixth Symposium (International) on Combustion*, The Combustion Institute, Pittsburgh, PA, pp. 347-355, 1996.
22. C. J. Mueller, J. F. Driscoll, D. L. Reuss, and M. C. Drake, "Vorticity Generation and Attenuation as Vortices Convect Through a Premixed Flame," *Combust. Flame* **112** , pp. 342-358, 1998.
23. W. L. Roberts and J. F. Driscoll, "A Laminar Vortex Interacting with a Premixed Flame: Measured Formation of Pockets of Reactants," *Combust. Flame* **87**, pp. 245-256, 1991.

24. W. L. Roberts, J. F. Driscoll, M. C. Drake, and J. W. Ratcliffe, "OH Fluorescence Images of the Quenching of a Premixed Flame During an Interaction with a Vortex," *Twenty-Fourth Symposium (International) on Combustion*, The Combustion Institute, Pittsburgh, PA, pp. 169-176, 1992.
25. W. L. Roberts, J. F. Driscoll, M. C. Drake, and L. P. Goss, "Images of the Quenching of a Flame by a Vortex--To Quantify Regimes of Turbulent Combustion," *Combust. Flame* **94**, pp. 58-69, 1993.
26. J. O. Sinibaldi, C. J. Mueller, A. E. Tulkki, and J. F Driscoll, "Suppression of Flame Wrinkling by Buoyancy: The Baroclinic Stabilization Mechanism," *AIAA J.* **36**, pp. 1432-1438, 1998.
27. J. O. Sinibaldi, C. J. Mueller, and J. F. Driscoll, "Local Flame Propagation Speeds Along Wrinkled, Unsteady, Stretched Premixed Flames," *Twenty-Seventh Symposium (International) on Combustion*, The Combustion Institute, Pittsburgh, PA, pp. 827-832, 1998.
28. P.-H. Renard, J. C. Rolon, D. Thevenin, and S. Candel, "Investigations of Heat Release, Extinction, and Time Evolution of the Flame Surface for a Non-Premixed Flame Interacting With a Vortex," *Combust. Flame* **117**, pp. 189-205, 1999.
29. J. C. Rolon, F. Aguerre, and S. Candel, "Experiments on the Interaction Between a Vortex and a Strained Diffusion Flame," *Combust. Flame* **100**, pp. 422-429, 1995.
30. D. Thevenin, P.-H. Renard, J. C. Rolon, and S. Candel, "Structure of a Nonpremixed Flame Interacting with Counterrotating Vortices," *Twenty-Sixth Symposium (International) on Combustion*, The Combustion Institute, Pittsburgh, PA, pp. 1079-1086, 1996.
31. D. Thevenin, P.-H. Renard, J. C. Rolon, and S. Candel, "Exctinction Processes During a Non-Premixed Flame/Vortex Interaction," *Twenth-Seventh Symposium (International) on Combustion*, The Combustion Institute, Pittsburgh, PA, pp. 719-726, 1998.
32. T. Takagi, Y. Yoshikawa, K. Yoshida, M. Komiyama, and S. Kinoshita, "Studies on Strained Non-Premixed Flames Affected by Flame Curvature and Preferential Diffusion," *Twenty-Sixth Symposium (International) on Combustion*, The Combustion Institute, Pittsburgh, PA, pp. 1103-1110, 1996.
33. K. Yosida and T. Takagi, "Transient Local Exctinction and Reignition Behavior of Diffusion Flames Affected by Flame Curvature and Preferential Diffusion," *Twenty-Seventh Symposium (International) on Combustion*, The Combustion Institute, Pittsburgh, PA, pp. 685-692, 1998.
34. V. S. Santoro, D. C. Kyritsis, and A. Gomez, "A Comparison of the Interaction of Laminar Vortices with Either Gaseous or Spray Counterflow Diffusion Flames," *First Joint Meeting of the United States Sections of the Combustion Institute*, Washington, DC, Paper No. 21, 1999.
35. K. Y. Hsu, Chen. L. D., V. R. Katta, L. P. Goss, and W. M. Roquemore, "Experimental and Numerical Investigations of the Vortex-Flame Interactions in a Driven Jet Diffusion Flame," *31st AIAA Aerospace Sciences Meeting & Exhibit*, Reno, NV, AIAA 93-0455, 1993.
36. V. R. Katta, K. Y. Hsu, and W. M. Roquemore, "Local Extinction in an Unsteady Methane-Air Jet Diffusion Flame," *Twenty-Seventh Symposium (International) on Combustion*, The Combustion Institute, Pittsburgh, PA, pp. 1121-1129, 1998.
37. R. D. Hancock, F. R. Schauer, R. P. Lucht, V. R. Katta, and K. Y. Hsu, "Thermal Diffusion Effects and Vortex-Flame Interactions in Hydrogen Jet Diffusion Flames," *Twenty-Sixth Symposium (International) on Combustion*, The Combustion Institute, Pittsburgh, PA, pp. 1087-1093, 1996.
38. C. J. Mueller and R. W. Schefer, "Coupling of a Diffusion Flame Structure to an Unsteady Vortical Flowfield," *Twenty-Seventh Symposium (International) on Combustion*, The Combustion Institute, Pittsburgh, PA, pp. 1105-1112, 1998.
39. S.-J. Chen and W. J. A. Dahm, "Diffusion Flame Structure of a Laminar Vortex Ring Under Microgravity Conditions," *Twenty-Seventh Symposium (International) on Combustion*, The Combustion Institute, Pittsburgh, PA, pp. 2579-2586, 1998.
40. Y. H. You, D. K. Lee, and H. D. Shin, "Visual Investigation of a Vortex Ring Interacting with a Nonpremixed Flame," *Combust. Sci. Technol.* **139**, pp. 365-383, 1998.
41. V. R. Katta and W. M. Roquemore, "Studies on Unsteady Opposing-Jet Diffusion Flames," *37th AIAA Aerospace Sciences Meeting and Exhibit*, Reno, NV, AIAA 99-0322, 1999.
42. M. Gharib, E. Rambod, and K. Shariff, "A Universal Time Scale for Vortex Ring Formation," *J. Fluid. Mech.* **360**, pp. 121-140, 1998.
43. W. T. Ashurst, "Flame Propagation Through Swirling Eddies, a Recursive Pattern," *Combust. Sci. Technol.* **92**, 87, 1993.
44. S. E. Widnall, "The Structure and Dynamics of Vortex Filaments," *Ann. Rev. Fluid. Mech.* **7**, pp. 141-165, 1975.
45. T. Poinsot, A. Trouve, D. Veynante, S. Candel, and E. Esposito, "Vortex-Driven Acoustically Coupled Combustion Instabilities," *J. Fluid Mech.* **177**, pp. 265-292, 1987.

46. C. J. Rutland and J. H. Ferziger, "Simulations of Flame-Vortex Interactions," *Combust. Flame* **84**, pp. 343-360, 1991.
47. H. N. Najm, P. H. Paul, C. J. Mueller, and P. S. Wyckoff, "On the Adequacy of Certain Experimental Observables as Measurements of Flame Burning Rate," *Combust. Flame* **113**, pp. 312-332, 1998.
48. P. H. Paul and H. N. Najm, "Planar Laser-Induced Fluorescence Imaging of Flame Heat Release Rate," *Twenty-Seventh Symposium (International) on Combustion*, The Combustion Institute, Pittsburgh, PA, pp. 43-50, 1998.
49. S. Gogineni, L. P. Goss, and W. M. Roquemore, "Manipulation of a Jet in a Cross Flow," *Exper. Therm. Fluid. Sci.* **16**, pp. 209-219, 1998.
50. S. Gogineni, L. Goss, D. Pestian, and R. Rivir, "Two-Color Digital PIV Employing a Single CCD Camera," *Exper. Fluids* **25**, pp. 320-328, 1998.
51. G. J. Fiechtner, C. D. Carter, V. R. Katta, J. R. Gord, J. M. Donbar, and J. C. Rolon, "Regimes of Interaction Between a Nonpremixed Hydrogen-Air Flame and an Isolated Vortex," *37th AIAA Aerospace Sciences Meeting and Exhibit*, Reno, NV, AIAA 99-0320, 1999.
52. A. Gomez and D. E. Rosner, "Thermophoretic Effects on Particles in Counterflow Laminar Diffusion Flames," *Combust. Sci. Technol.* **89**, pp. 355-362, 1993.
53. C. J. Sung, J. S. Kistler, M. Nishioka, and C. K. Law, "Further Studies on Effects of Thermophoresis on Seeding Particles in LDV Measurements of Strained Flames," *Combust. Flame* **105**, pp. 189-201, 1996.